CHEMISTRY
A EUROPEAN JOURNAL

DOI: 10.1002/chem.201003613

A Series of Tripodal Cysteine Derivatives as Water-Soluble Chelators that are Highly Selective for Copper(I)

Anaïs M. Pujol, Christelle Gateau, Colette Lebrun, and Pascale Delangle*[a]

Abstract: A series of tripodal ligands derived from nitrilotriacetic acid and extended by three converging, metal-binding, cysteine chains was synthesised. Their ability to bind soft metal ions thanks to their three thiolate functions was investigated by means of complementary analytical and spectroscopic methods. Three ligands that differ by the nature of the carbonyl group next to the coordinating thiolate functions were studied: $\mathbf{L^1}$ (ester), $\mathbf{L^2}$ (amide) and $\mathbf{L^3}$ (carboxylate). The negatively charged derivative $\mathbf{L^3}$, which bears three carboxylate functions close to the metal binding site, gives polynuclear copper(I) complexes of low stability. In contrast, the ester and amide derivatives $\mathbf{L^1}$ and $\mathbf{L^2}$ are efficient Cu^I chelators with very high affinities, close to that reported for the metal-sequestering metallothioneins ($\log K \approx 19$). Interestingly, these two ligands form mononuclear copper complexes with a unique MS_3 coordination in water solution. An intramolecular hydrogen-bond network involving the amide functions in the upper cavity of the tripodal ligands stabilises these mononuclear complexes and was evidenced by the very low chemical-shift temperature coefficient of the secondary amide protons. Moreover, $\mathbf{L^1}$ and $\mathbf{L^2}$ display large selectivities for the targeted metal ion that is, Cu^I, with respect to bioavailable Zn^{II}. Therefore the two sulfur-based tripods $\mathbf{L^1}$ and $\mathbf{L^2}$ are of potential interest for intracellular copper detoxication in vivo, without altering the homeostasis of the essential metal ion Zn^{II}.

Keywords: bioinorganic chemistry · chelating agents · copper · ligands · selectivity

Introduction

Metallic elements play major roles in biochemistry. The essential transition-metal ions are used by cells in structurally constrained binding sites in metalloproteins, in which they can carry out structural, regulatory or catalytic roles. As these metal ions can also catalyse cytotoxic reactions, several families of proteins are present in cells to control their concentration and to confine them to vital roles.[1–4]

Among essential metallic elements, copper is used as cofactor in many redox proteins involved in several vital processes. Free copper can also promote Fenton-like reactions and would thus be very toxic even at low concentration. Therefore intracellular copper concentration needs to be rigorously controlled so that it is only provided to the essential enzymes, but does not accumulate to toxic levels.[3–6] Wilson's disease is one of the major genetic disorder of copper metabolism in humans. Impairment of copper transport in hepatocytes results in cytosolic copper accumulation with associated cellular injury.[7,8] Copper is also involved in neurodegenerative diseases like Alzheimer's disease and suspected to cause Aβ precipitation and toxicity.[9,10] Chelation therapy[8,9,11] is currently used or proposed for treating these disorders and intoxication, therefore it is of major interest to develop molecules able to efficiently and selectively bind copper. In particular, intracellular copper chelation would be an efficient tool to remove metal ions from organs where it is accumulated.[12]

As the cytoplasm of most eukaryotic cells is a reducing environment, the predominant oxidation state of copper in cells is Cu^I,[7] which has a soft character and thus a high affinity for soft donors like thiolates. This preference for soft sulfur ligands is exemplified in proteins involved in copper homeostasis,[3] which mainly bind these ions with several thiolates of cysteine side chains. Many intracellular Cu transporters contain a conserved N-terminal MxCxxC sequence that binds metal ions with two cysteines.[13] In a previous report, the model cyclodecapeptide $\mathbf{P^C}$, c(MTCGSCSRP), incorporating the binding sequence (MTCSGC) of the yeast copper chaperone Atx1 was found highly selective for Cu^I and Hg^{II} with respect to Zn^{II}, another essential metal ion found in cells.[14,15] Therefore, a glycopeptide also containing two cysteines and targeted at the hepatocytes was recently designed and demonstrated to be able to chelate intracellular copper. This compound may be a good candidate to fight copper overload in the liver.[12]

Metallothioneins (MT) are other proteins that sequester many metals, in particular Cu and Zn with a higher affinity for Cu^I. When copper is in excess of physiological require-

[a] Dr. A. M. Pujol, Dr. C. Gateau, C. Lebrun, Dr. P. Delangle
INAC
Service de Chimie Inorganique et Biologique (UMR E3 CEA UJF)
Commissariat à l'Energie Atomique, 17 rue des martyrs
38054 Grenoble cedex (France)
Fax: (+33) 438785090
E-mail: pascale.delangle@cea.fr

Supporting information for this article is available on the WWW under http://dx.doi.org/10.1002/chem.201003613.

ments, cells induce the biosynthesis of these small cysteine-rich proteins, which form metal clusters.[16,17] Indeed, MTs interact very efficiently with Cu^{I} in thiolate-rich environments and the crystal structure of the yeast copper thionein (Cu_8-MT) shows that two copper ions are digonally coordinated to cysteine residues, whereas the six other copper ions are trigonally bound, in a Cu_8-thiolate cluster.[18] This suggests that the trithiolato trigonal coordination affords stable complexes of Cu^{I}.

To design efficient and selective soft metal ion chelators, we take advantage of the high affinity of cysteine sulfur donors for Cu^{I}, evidenced in proteins trafficking or sequestering this metal in cells.[12,14,15,19] As trithiolato coordination environments afford very stable Cu^{I} complexes in metallothioneins, ligands with three cysteine residues that promote a MS_3 geometry are very attractive. Therefore, three cysteine moieties can be attached with peptide bonds to non-biological scaffolds to get pseudopeptide ligands.[20] Indeed, chemical scaffolds can serve as platforms for the design of podands that have all their binding arms oriented in the same direction to coordinate metal ions.[21] We have used such a strategy to obtain polydentate metal complexing molecules by appending several chelating functions in the same chemical architecture.[22] Polyaminocarboxylates provide a series of chemical scaffolds with a range of carboxylic acids numbers that can be easily functionalised with cysteines. Following this strategy, we have recently demonstrated that a first tripodal cysteine-based ligand, namely $\mathbf{L^1}$, anchored on a nitrilotriacetic acid (NTA) moiety, chelates very efficiently Cu^{I} and Hg^{II}.[19]

Here we report on a series of tripodal ligands extended by three converging metal-binding cysteine chains. To test the effect of the carbonyl function near to the coordinating sulfur group, we synthesised the three derivatives $\mathbf{L^{1-3}}$ shown here. The coordination properties of these ligands were investigated by means of complementary analytical and spectroscopic methods. The results presented in this article show that the nature of the carbonyl function next to the thiols influences the complexation properties. The ester and amide derivatives $\mathbf{L^1}$ and $\mathbf{L^2}$ are efficient Cu^{I} chelators with very high affinities. The formation of mononuclear copper complexes with a unique MS_3 coordination in water is especially attractive. Moreover these ligands display large selectivities for the targeted metal ion that is, Cu^{I}, with respect to bioavailable Zn^{II}. Therefore these two compounds are of potential interest for metal detoxication in vivo, without altering the homeostasis of the essential metal ion Zn^{II}.

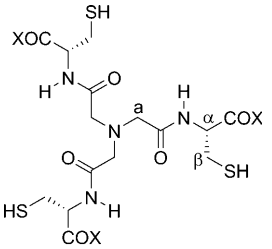

$H_3\mathbf{L^1}$: X = OEt
$H_3\mathbf{L^2}$: X = NH_2
$H_6\mathbf{L^3}$: X = OH

Results

Syntheses and characterisation of the three ligands: The synthetic procedures of the ligands $\mathbf{L^{1-3}}$ are summarised in Scheme 1. The three pseudopeptides were synthesised from nitrilotriacetic acid (NTA). The first step is the coupling of the free amine group of the S-protected cysteine derivatives H-Cys(Trt)-OEt or H-Cys(Trt)-NH_2 to the carboxylic acid functions of NTA in presence of classical peptide-synthesis coupling agents to afford the tripodal precursors **1** and **2** in good yields. Then the thiol groups were deprotected under acidic conditions to give $\mathbf{L^1}$ and $\mathbf{L^2}$. The ligand $\mathbf{L^3}$ was obtained in two steps from compound **1**, the ester functions of which were first hydrolysed into acids with lithium hydroxide. Then the thiol groups were deprotected under acidic conditions to afford $\mathbf{L^3}$ as a white solid. The ligands $\mathbf{L^{1-3}}$ were purified by RP18 HPLC and obtained with overall yields from NTA of 40, 34 and 60%, respectively. These

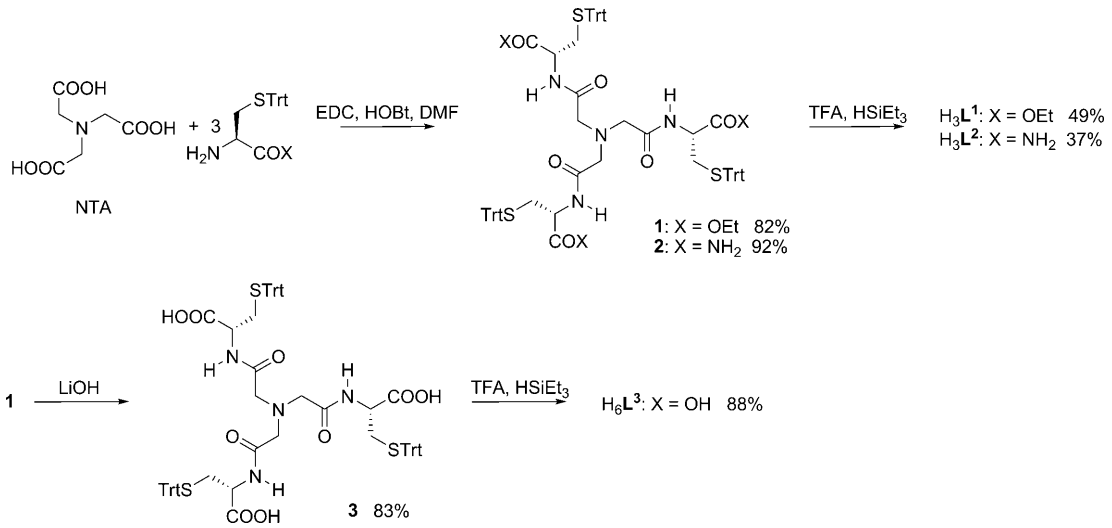

Scheme 1. Syntheses of the three ligands $\mathbf{L^{1-3}}$.

thiol-containing compounds are oxygen-sensitive and were stored and manipulated in a glove box in an argon atmosphere.

The proton and carbon NMR spectra of each ligand indicate the presence of a single C_3-symmetric species in which the three arms are equivalent. The apical $N-CH_2$ methylene protons give well-resolved AB doublets and the β-protons of cysteines characteristic ABX systems.

Potentiometric studies were conducted in KCl 0.1 M at 298 K to determine the protonation constants of the thiol groups in the ligands. The protonation constants, K_H^i, are defined in Equation (1) and could be obtained from the titrations of the compounds with KOH and HCl. The results are listed in Table 1.

Table 1. Protonation constants of the ligands $\mathbf{L^{1-3}}$ from potentiometric measurements in water KCl 0.1 M at 298 K.

Ligand	$\mathbf{L^1}$	$\mathbf{L^2}$	$\mathbf{L^3}$
pK_{a1}	9.4	10.2	10.6
pK_{a2}	9.0	9.2	10.0
pK_{a3}	8.1	8.5	9.2
pK_{a4}	<2.8	2.8	3.8
pK_{a5}	–	–	3.3
pK_{a6}	–	–	2.8

$$LH_{i-1} + H \rightarrow LH_i$$
$$K_H^i = [LH_i]/[LH_{i-1}][H] \qquad pK_{ai} = \log K_H^i \tag{1}$$

The pH titrations of $\mathbf{L^1}$ and $\mathbf{L^2}$ are indicative of three weak acidic sites (Figure S1 in the Supporting Information), corresponding to the deprotonation of the thiol functions ($pK_a = 8–10$). A fourth protonation constant is necessary to fit the titration of $\mathbf{L^2}$ and corresponds to the protonation of the apical nitrogen at low pH. The fourth pK_a of $\mathbf{L^1}$ could not be fitted, probably because it is lower than the pH range explored in the titration experiments (pH > 2.8). The unusually low value of the apical amine pK_a is consistent with the value published for another tripodal compound with an apical nitrogen atom substituted with three amide groups (N-$(CH_2CONH_2)_3$, $pK_a = 2.6$).[23] As expected, the pH titration of $\mathbf{L^3}$ is indicative of six weak acidic sites. The three highest pK_a's are in the range of thiol deprotonation, whereas the three lowest are characteristic of carboxylic acid deprotonations.

The values of the thiol protonation constants indicate that the acid ligand $\mathbf{L^3}$ ($\Sigma pK_a^{SH} = 29.8$) is more basic than the amide derivative $\mathbf{L^2}$ ($\Sigma pK_a^{SH} = 27.9$), which is also more basic than the ester derivative $\mathbf{L^1}$ ($\Sigma pK_a^{SH} = 26.5$). This evolution reflects the electron-withdrawing characters of the carbonyl functions close to the thiol, which range in the order ester > amide > carboxylate. The same tendencies were already observed for small peptides containing cysteines.[24]

UV and CD titrations with Cu^I: Binding of Cu^I was investigated by UV and CD spectroscopy. It is known that Cu^I disproportionates in Cu^0 and Cu^{II} in water. Therefore the experiments with this cation were conducted in the presence of acetonitrile, which associates with Cu^I and overcomes the disproportionation reaction.[25] Binding of Cu^I to $\mathbf{L^{1-3}}$ was first monitored by UV spectroscopy. The addition of aliquots of tetrakis(acetonitrile) copper (I) hexafluorophosphate dissolved in acetonitrile over a peptide solution in a 9:1 (v/v) mixture of phosphate buffer (20 mM, pH 7.4) and acetonitrile displays the appearance of a band centred at 267 nm that linearly increases with increasing Cu^I concentration up to two equivalents. This band is characteristic of charge-transfer transitions (LMCT) of thiolate–Cu^I bonds, as well as for divalent d^{10} metal ions like Hg^{II} or Zn^{II}.[26,27] The extinction coefficient of this LMCT bands are in the range expected for the coordination of two Cu^I ions, found in MT of ≈7000 per Cu bound.[26]

Titrations with the ester and amide derivatives $\mathbf{L^1}$ and $\mathbf{L^2}$ give very similar results and the example of $\mathbf{L^2}$ is presented in Figure 1. These titrations suggest the formation of two

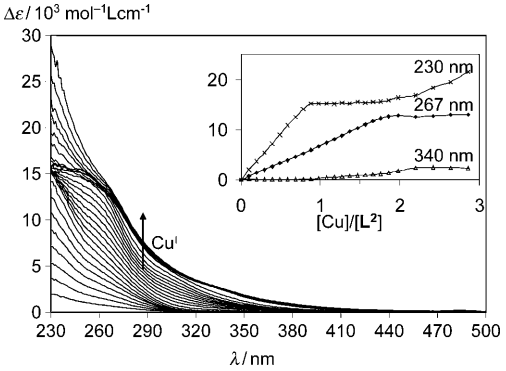

Figure 1. UV titration of $\mathbf{L^2}$ (≈50 μM) with Cu^I at pH 7.4 (20 mM phosphate buffer/CH_3CN (v/v = 9:1)). Spectra shown are difference spectra [$\Delta\varepsilon = \varepsilon(Cu\mathbf{L^2}) - \varepsilon(\mathbf{L^2})$] and correspond to samples with 0–3 equivalents of Cu^I per $\mathbf{L^2}$.

different types of complexes: a mononuclear complex when less than one Cu equivalent is added and polynuclear complexes when more than one Cu equivalent is added. Indeed up to the addition of one equivalent of Cu, a high-energy band develops with an absorption maximum below 230 nm. No low-energy band, attributed to cluster-centred transitions[26,27] around 340 nm is detected. CD titrations also evidence the formation of a unique complex when less than one equivalent of Cu is added, with intense dichroic bands with positive and negative maxima (see Table 2), and no CD signal characteristic of cluster-centred transitions. Besides, three isodichroic points are evidenced in the CD titrations between the addition of 0 and one equivalents of copper, as seen in Figure 2 (left) demonstrating that the free ligand is in equilibrium with a unique copper species. The mononuclear complexes Cu-$\mathbf{L^1}$ and Cu-$\mathbf{L^2}$ are also nicely evidenced in the ES-MS spectra, which show intense peaks at $m/z = 645$ $[Cu\mathbf{L^1}H]^-$ and 558 $[Cu\mathbf{L^2}H]^-$. These data are consistent with the formation of mononuclear Cu^I complexes with LMCT absorption bands at higher energy (≈230 nm)

Table 2. UV and CD characteristics of Cu^{I} complexes at pH 7.4 (20 mM phosphate buffer/CH_3CN (v/v = 9/1)).

	UV λ [nm] (ε [$mol^{-1}Lcm^{-1}$])	CD
Cu-$\mathbf{L^1}$	230 (14300)	237 (−)
	267 (7200)	262 (+), 288(−)
	340 (40)	
$(Cu_2\text{-}\mathbf{L^1})_3$	230 (15000)	235 (−)
	267 (13500)	259 (+), 284(−)
	340 (2500)	310 (−) 340(+)
Cu-$\mathbf{L^2}$	230 (17600)	222 (+)
	266 (7900)	253 (−), 279(+)
	340 (20)	
$(Cu_2\text{-}\mathbf{L^2})_x$	230 (17600)	220 (+)
	266 (13500)	258 (−), 291(−)
	340 (2600)	313 (−) 341(+)
$(Cu_2\text{-}\mathbf{L^3})_x$	230 (17000)	226 (+)
	267 (12200)	256 (−), 278 (−)
	340 (1350)	343 (+)

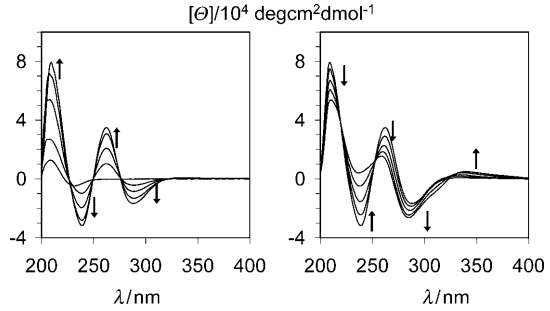

Figure 2. CD titration of $\mathbf{L^1}$ (≈50 μM) with Cu^{I} at pH 7.4 (20 mM phosphate buffer/CH_3CN (v/v = 9:1)). Left: 0–1 equivalents Cu. Right: 1–2 equivalents of Cu.

than in copper clusters (≈260 nm).[27] Besides, in solutions of Cu-$\mathbf{L^{1,2}}$ in a 9:1 (v/v) mixture of phosphate buffer (20 mM, pH 7.4) and acetonitrile, the cysteine free-thiol concentration, measured following Ellman's procedure[28] is insignificant, which demonstrates that the three thiolate functions of the ligand are coordinated to the Cu^{I} ion in a mononuclear CuS_3 coordination environment.

When an excess of Cu^{I} is used with respect to $\mathbf{L^1}$ and $\mathbf{L^2}$, the UV and CD features change dramatically and indicate the formation of Cu^{I} polymetallic species. In the UV spectra, the high-energy band around 230 nm attributed to the CuS_3 mononuclear centre reaches a plateau at the addition of one to two equivalents of Cu and weak, low-energy contributions (around 340 nm) appear. These weak low-energy bands also appear in the CD spectra with maxima at 310 and 340 nm as seen in Figure 2 (right) and are attributed to cluster-centred transitions.[26,27] Going from one to two equivalents of Cu^{I}, several isodichroic points are detected in the CD spectra obtained with both ligands $\mathbf{L^1}$ and $\mathbf{L^2}$, demonstrating that the mononuclear complex Cu-$\mathbf{L^{1,2}}$ is transformed into a single cluster complex $(Cu_2\text{-}\mathbf{L^{1,2}})_x$. The cluster $(Cu_2\mathbf{L^1})_3$ was previously identified by ES-MS.[19]

The titration of the acid derivative $\mathbf{L^3}$ with Cu^{I} show a different behaviour than those observed with $\mathbf{L^1}$ and $\mathbf{L^2}$. Indeed, low-energy bands around 340 nm are detected at the beginning of UV (Figure S2 in the Supporting Information) and CD titrations ($\Delta\varepsilon_{(340\,nm)} \approx 1000\ mol^{-1}Lcm^{-1}$ for 1 equiv Cu). This exemplifies the formation of polynuclear copper complexes even in excess of $\mathbf{L^3}$. Besides, the high-energy band around 230 nm increases linearly with increasing Cu^{I} concentration and does not show any endpoint at the addition of one equivalent of Cu, as observed with $\mathbf{L^1}$ and $\mathbf{L^2}$. The presence of the carboxylate functions in $\mathbf{L^3}$ at pH 7.4 disfavours the formation of the mononuclear copper complex.

^{1}H NMR spectra of Cu-$\mathbf{L^{1,2}}$: The Cu^{I} complexes of $\mathbf{L^3}$ give poorly resolved ^{1}H NMR spectra and were not extensively studied. In contrast, the ^{1}H NMR spectra of $\mathbf{L^1}$ and $\mathbf{L^2}$ in presence of Cu^{I} show the formation of a C_3-symmetric complex for less than one metal equivalent (Figure 3). The equilibrium between the free ligand and the complex is slow on the NMR time scale at 500 MHz. In these complexes, the chemical shift differences between the two β-protons of the cysteines (ABX spin system) and of the apical NCH_2 protons (AB spin system) are greatly enhanced with respect to the free ligand, which suggests that the ligands adopt rigid conformations in the metal complex with the three thiolate arms wrapped around the metal ion. A closer look to the ABX spin system of the β-protons of the cysteines indicates that the conformation around the C_α–C_β bonds of the cys-

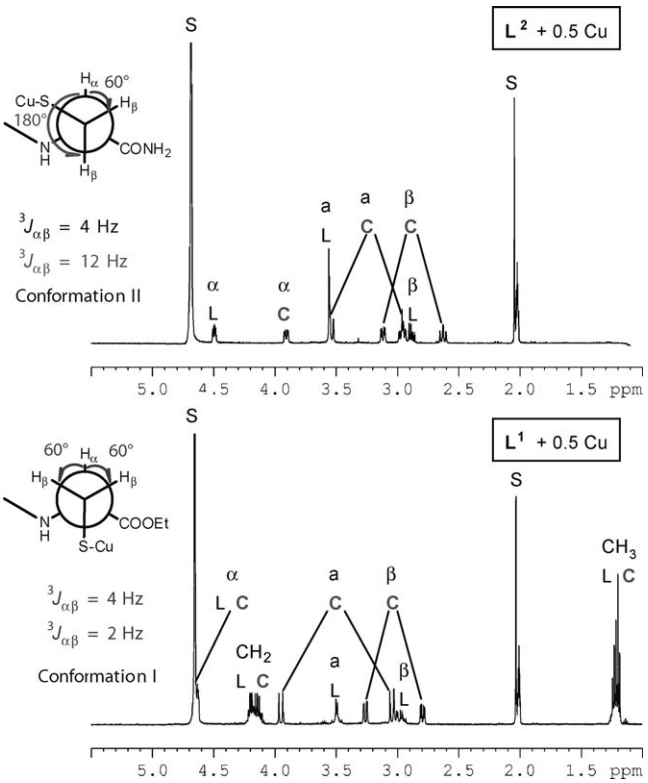

Figure 3. 500 MHz ^{1}H NMR spectra of $\mathbf{L^1}$ and $\mathbf{L^2}$ with 0.5 equivalents of $Cu(CH_3CN)_4.PF_6$ at pD 7.4 (20 mM phosphate buffer in D_2O/CD_3CN (v/v=9:1) at 298 K. L and C mean the free ligand and the Cu-**L** complex, respectively.

teine residues is different for the two copper complexes. Indeed for Cu-$\mathbf{L^1}$, the values of the ^3J coupling constants are 4 and 2 Hz, characteristic of $H_\alpha CCH_\beta$ dihedral angles of about 60° from the Karplus equation[29] (conformation I, Figure 3). In contrast, the patterns are totally different for Cu-$\mathbf{L^2}$ with two very different ^3J coupling constants (4 and 12 Hz) characteristic of $H_\alpha CCH_\beta$ dihedral angle values of approximately 60 and 180° (conformation II, Figure 3). Furthermore, the α-proton is especially shielded in Cu-$\mathbf{L^2}$ (3.9 ppm instead of 4.5 ppm in the free ligand or 4.6 ppm in Cu-$\mathbf{L^1}$), because the metal ion is closer to this proton in conformation II.

The diffusion coefficients were measured by pulsed gradient spin echo (PGSE) NMR to infer the species molecularity in solution.[30] This method has proved to be a useful tool for probing the presence of unimolecular, bimolecular or oligomeric species in solution.[31] Indeed, the diffusion constant D can be related to the hydrodynamic radii of the molecules by the Stokes–Einstein equation [Eq. (2)] in which k is the Boltzmann constant, T the absolute temperature, η the viscosity and r_H the hydrodynamic radius of the diffusing species, considered as a hypothetical hard sphere that diffuses with the same speed as the particle under examination.

$$D = \frac{kT}{6\pi\eta r_H} \tag{2}$$

The determination of D by diffusional NMR spectroscopy for shape-similar complexes and ligands is thus an efficient tool for deducing the molecular mass of an unknown species (i, molar mass M_i) in solution, when a reference compound (r, molar mass M_r) is measured under the same conditions [Eq (3)].[30]

$$\frac{D_i}{D_r} = \sqrt[3]{\frac{M_r}{M_i}} \tag{3}$$

The experimental diffusion coefficients and the calculated mass of the complexes (M_{diff}) are presented in Table 3. The reference compound used for the mass calculation in Equation (3) is the free ligand in the same solvent. As seen in Table 3, these results confirm the formation of copper mononuclear complexes Cu-$\mathbf{L^1}$ and Cu-$\mathbf{L^2}$.

Table 3. Translational diffusion coefficients measured by PFG-1H NMR at 298 K in phosphate buffer (20 mM, D_2O, pD 7.4)/CD_3CN v/v = 9:1. Experimental errors on the last character are indicated in parentheses.

	D $[m^2 s^{-1} mol^{-1}] \times 10^{10}$	M_{diff} $[g mol^{-1}]$[a]	$M_{formula}$ $[g mol^{-1}]$[b]
$\mathbf{L^1}$	3.20(4)	–	585
Cu-$\mathbf{L^1}$	3.02(4)	700(50)	645
Pb-$\mathbf{L^1}$	3.1(1)	650(90)	789
Zn-$\mathbf{L^1}$, (Zn-$\mathbf{L^1}$)$_2$	2.80(4)	870(70)	647, 1292
(Cd-$\mathbf{L^1}$)$_2$	2.4(1)	1400(200)	1386
$\mathbf{L^2}$	3.40(4)	–	498
Cu-$\mathbf{L^2}$	3.30(4)	545(40)	558
Pb-$\mathbf{L^2}$	3.20(5)	600(50)	701
Zn-$\mathbf{L^2}$	2.8(1)	890(120)	559, 1118
(Cd-$\mathbf{L^2}$)$_2$	2.5(1)	1250(200)	1212

[a] Molecular mass calculated with Equation (3), reference compound is the free ligand. [b] Molecular mass calculated with the chemical formula of the species.

As we suspected a network of hydrogen bonds involving the amide functions of the "upper cavity" ($NH_{arm(i)}\cdots O{=}C_{arm(i+1)}$), we investigated the temperature coefficients of the amide proton resonances in H_2O/D_2O (v/v = 90:10). Indeed, intermolecular hydrogen bonds and those to the solvent are readily cleaved with increasing temperature, which leads to large temperature coefficients. In contrast, it is generally assumed that NHs with temperature gradients less negative than -3 ppb °C^{-1} are solvent-shielded in stable peptide structures, and indicate intramolecular hydrogen bonding.[32] The temperature coefficients of the secondary amide proton resonances of the two complexes Cu-$\mathbf{L^1}$, and Cu-$\mathbf{L^2}$ are reported in Table 4, with those of the free ligands for comparison. As expected, the temperature coefficients of the amide protons of the two ligands are large, because these protons strongly interact with the solvent in the flexible structures of the free tripods. In contrast, the chemical shift variations of complexes are close to zero, which evidences intramolecular hydrogen bonds involving the amide protons of the "upper cavity". The C_3-symmetrical structures of the metal complexes were built in Chem3D by imposing a trigonal planar coordination to Cu^I with S–Cu distances of 2.25 Å.[33] As expected in these structures, the three peptide bonds of the "upper cavity" are likely to form intramolecular H-bonds involving the NH of one arm and the CO of the next arm (Figure 4). The H···O, N···O distances are 3.1 and 3.9 Å, respectively and the N–H···O angle is 137°, characteristic of weak hydrogen bonds.[34] Of course, NMR experiments do not allow us to discriminate between the C_3-symmetrical structure with three weak hydrogen bonds like in Figure 4 and a nonsymmetrical structure with only two strong hydrogen bonds, which would be dynamic on the NMR timescale providing an average C_3-symmetrical species spectrum. The hydrogen-bond network probably contributes to the stabilisation of the mononuclear copper complexes of $\mathbf{L^1}$ and $\mathbf{L^2}$.

Table 4. Temperature coefficients of the amide proton resonances, in phosphate buffer (20 mM, pH 7.4)/CD_3CN, 90/10 (v:v).

	$-\Delta\delta/\Delta T$ [ppb per °C]	
	$\mathbf{L^1}$	$\mathbf{L^2}$
Free L	6.8	6.5
Cu**L**	0.8	0.1

In an excess of Cu^I, the ^{1}H NMR spectra of $\mathbf{L^1}$ and $\mathbf{L^2}$ complexes broaden, which was assigned to the formation of higher nuclearity species, experiencing intramolecular dynamics associated with exchange of the sulfur ligands from one Cu ion to another. Besides, these polynuclear complexes were also evidenced above with UV and CD spectroscopy. The diffusion coefficient of $(Cu_2\text{-}\mathbf{L^1})_x$ could be precisely measured thanks to the ^{1}H NMR resonances of the ethyl groups of the ester functions. The diffusion coefficient, $D_{(Cu_2\text{-}\mathbf{L^1})_x} = 2.0(1) \times 10^{-10}$ m^2 s^{-1}, confirms the trimeric nature

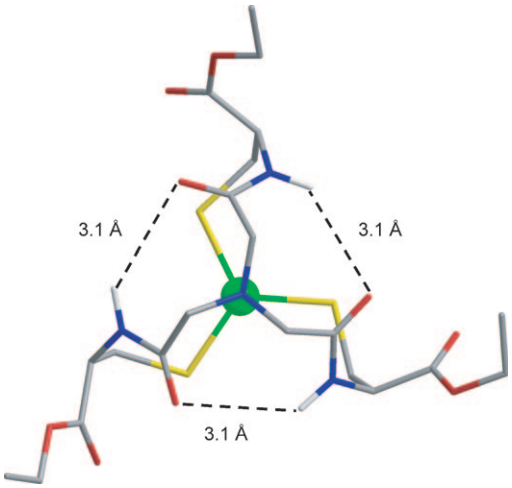

Figure 4. C_3-symmetrical structure of Cu-**L**^{1} showing the hydrogen bonds in the "upper cavity". C: grey, H: white, O: red, N: blue, S: yellow, Cu: green.

of this complex and gives $M_{(Cu_2L)_x} \approx 2200(400)\ g\,mol^{-1}$ and therefore $x=3$. The polymetallic complex Cu_6-$\mathbf{L}_3$ can be associated with a Cu_6S_9 core as described in some metallothioneins, in which all of the Cu^I adopts nearly trigonal planar coordination with exclusively bridging thiolates.[35]

Pb, Cd and Zn complexes of L$^{1-3}$: The titrations of **L**^{1} and **L**^{2} with Pb^{II}, Cd^{II} and Zn^{II} show sharp endpoints for the addition of one equivalent of metal ion with the appearance of charge-transfer transitions (LMCT) due to the thiolate–M^{II} bonds. Typical titrations are presented in Figure 5 for ligand **L**^{2}. As seen in Table 5, the LMCT bands, in particular the extinction molar coefficients are consistent with metal ions coordinated with the three thiolates of the ligand. Indeed, Godwin et al. characterised tristhiolato–lead complexes with absorption bands at about 335 nm with $\varepsilon \approx 4000\ mol^{-1}\,L\,cm^{-1}$.[36] Well-defined tristhiolato cadmium

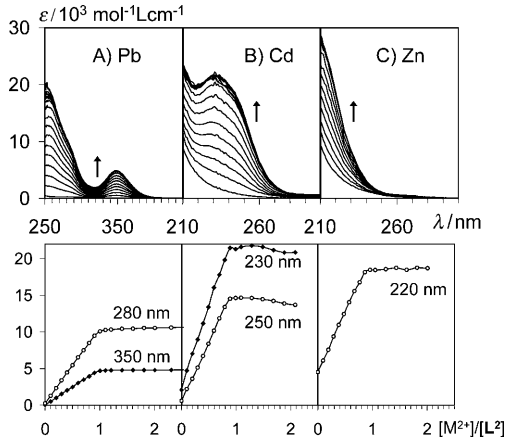

Figure 5. UV titration of **L**^{2}. A) (65 μM) with Pb^{II} in Bis-Tris buffer (20 mM, pH 7), B) (32 μM) with Cd^{II} in phosphate buffer (20 mM, pH 7.4) and C) (32 μM) with Zn^{II} in phosphate buffer (20 mM, pH 7.4) with 0–2 equivalents of metal per **L**^{2}.

Table 5. Characteristics of the LMCT bands of Zn, Cd and Pb complexes in phosphate buffer (20 mM, pH 7.4) for Zn and Cd and in Bis-Tris buffer (20 mM, pH 7) for Pb. $\Delta\varepsilon = \varepsilon(ML^i) - \varepsilon(L^i)$.

	UV λ [nm] ($\Delta\varepsilon$ [mol^{-1} L cm^{-1}])		
	L^1	**L**^{2}	**L**^{3}
Zn^{II}	210, (21500)	210 (22600)	210 (17250)
Cd^{II}	230 (20000)	230 (22000)	227 (21500)
Pb^{II}	350 (5500)	350 (4900)	350 (4900)[a]

[a] For the Pb/**L**^{3} system, higher energy bands develop in excess of Pb^{II} with an absorption maximum at 215 nm.

complexes described by Pecoraro et al. show absorption data very close to ours ($\lambda_{max} \approx 230$ nm and $\varepsilon \approx 20000$–$22000\ mol^{-1}\,L\,cm^{-1}$).[37] Besides, Vasak et al. determined an averaged contribution per S–Cd bond of 5500–$6500\ mol^{-1}\,L\,cm^{-1}$.[38]

The ^{1}H NMR spectra of these complexes are very similar to those of Cu^I and indicate the formation of C_3-symmetric species (Figure S3 in the Supporting Information). They show large NMR resonances for the addition of less than one equivalent of metal, indicating that free ligand–complex equilibria are more rapid on the NMR timescale with these divalent ions than with Cu^I. Interestingly, the diffusion coefficients indicate important differences for the coordination complexes of the three metal ions (Table 3). Whereas Pb^{II} forms mononuclear complexes Pb-**L** with a PbS_3 environment, Cd^{II} forms dinuclear complexes Cd_2-$\mathbf{L}_2$ with **L**^{1} and **L**^{2}. The formation of a dimeric cadmium complex has already been observed with a peptide modelling APP ($APP^{170-188}$) which contains also three cysteine residues.[39] This dimer contains a dinuclear cluster in which two divalent Cd^{II} are bridged by two thiolate ligands from cysteine residues. The tetrahedral coordination sites of each metal ion are completed by nonbridging thiolate ligands as represented in Scheme 2. The formation of a unique complex was confirmed by the CD titrations with **L**^{1} and **L**^{2}, which show the transformation of the ligand into one unique metal species with two dichroic bands (210(+) and 248(−)) and an isodicroic point at 233 nm (Figure S4 in the Supporting Information). According to diffusion data, this unique complex was attributed to Cd_2-$\mathbf{L}_2$. The diffusion coefficients measured for the zinc complexes are in between those expected for mono and dimeric species, suggesting equilibrium between the two complexes Zn-**L** and Zn_2-$\mathbf{L}_2$. ES-MS titrations of **L**^{1} and **L**^{2} with these divalent metal ions evidence mainly the monomolecular species M-**L**, but weak signals corresponding to the bimolecular species M_2-$\mathbf{L}_2$ are also seen in the ES-MS spectra of cadmium complexes. Surprisingly, all these complexes give nice ^{1}H NMR spectra indicative of C_3 symmetry, even though the species M_2-$\mathbf{L}_2$ has lower symmetry. This demonstrates that the intramolecular dynamics in the dimer is very rapid on the NMR

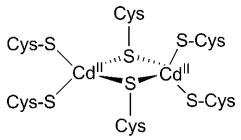

Scheme 2. Schematical representation of the dimer Cd_2S_6.

timescale and prevents the observation of the real symmetry of the complex.

The ligand $\mathbf{L^3}$ gives similar UV titrations to $\mathbf{L^1}$ and $\mathbf{L^2}$ with Cd and Zn. In contrast with Pb^{II}, the UV spectra evolve significantly after one equivalent of Pb is added (Figure S5 in the Supporting Information). A first LMCT band grows until the addition of one equivalent of Pb, with the same characteristic as Pb-$\mathbf{L^1}$ and Pb-$\mathbf{L^2}$, indicative of a PbS_3 environment. Then a second more intense LMCT band appears at lower energy (315 nm) characteristic of a lower number of coordinated thiolate functions.[14] This singular behaviour was assigned to the coordination of the non innocent acetate function in a five-membered chelate ring which is observed only for the large borderline ion Pb^{II}. These titrations are perfectly fitted with the successive formation of Pb-$\mathbf{L^3}$ (340 nm, 4900 $mol^{-1}Lcm^{-1}$), $Pb_2\mathbf{L^3}$(315 nm, 6800 $mol^{-1}Lcm^{-1}$) and Pb_3-$\mathbf{L^3}$ (315 nm, 11 000 $mol^{-1}Lcm^{-1}$) as shown in the Supporting Information.

Affinities and selectivities: The affinity of the three tripods for Cu^I was evaluated at physiological pH, by UV/Vis titrations in presence of a chelator of known affinity. Bathocuproine disulfonate (Na_2BCS) has been demonstrated to form a stable 1:2 complex, $Cu(BCS)_2^{3-}$, according to Equation (4) with a constant, $\log\beta_{12}=19.8$.[40]

$$Cu^+ + 2\,BCS^{2-} \rightarrow [Cu(BCS)_2]^{3-} \quad (4)$$

The complex $[Cu(BCS)_2]^{3-}$ exhibits an absorption band in the visible region with its maximum at 483 nm ($\varepsilon=13300\,M^{-1}cm^{-1}$). Addition of BCS to a solution of Cu-$\mathbf{L^i}$ in a 9:1 (v/v) mixture of phosphate buffer (20 mM, pH 7.4) and acetonitrile shows the appearance of the absorption band of $[Cu(BCS)_2]^{3-}$, which corresponds to the transfer of the metal cation from the tripod to BCS^{2-}. Figure 6 displays the quantity of BCS required to displace 50% of Cu from the Cu^I complex of $\mathbf{L^i}$. Ligand $\mathbf{L^1}$ has the highest affinity for Cu^I as 80 equivalents of BCS are required to remove 50% of Cu^I from the complex. In comparison, $\mathbf{L^3}$ is a poor ligand as only 2.5 equivalents of BCS displace 50% of the Cu. Titrations of $\mathbf{L^1}$ and $\mathbf{L^2}$, preloaded with 0.8–0.9 equivalents of Cu^I to form the mononuclear complex, with aliquots of the competitor (BCS^{2-}) solution could be fitted according to Equation (5) with very high conditional stability constants ($\log K \approx 19$) reported in Table 6. The measurements were performed with a range of BCS concentrations and gave the same constant according to Equation (5), which demonstrates the absence of ternary species with BCS. It appears clearly that the two ligands $\mathbf{L^1}$ and $\mathbf{L^2}$ are very efficient copper complexing agents with affinities somewhat higher than those reported for a model peptide of Atx1 ($\log K=17.4$ at pH 7.4)[14,15] or for the whole Atx1 protein.[40,41] These very large conditional stability constants are of the same order of magnitude as the one found in metallothioneins.[17]

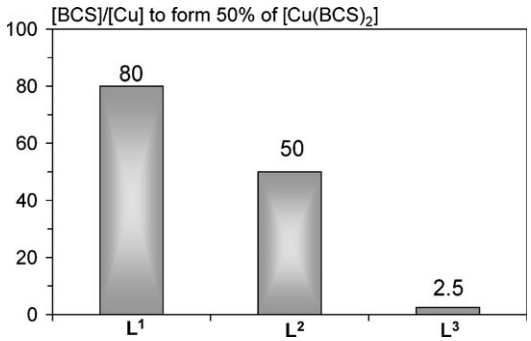

Figure 6. Number of BCS equivalents per Cu, required to form 50% of $[Cu(BCS)_2]$ from samples containing [Cu] = 0.8 [$\mathbf{L^i}$] and [$\mathbf{L^i}$] = 50 μM in 20 mM phosphate buffer, pH 7.4 at 298 K, acetonitrile 9:1 v/v.

Table 6. Conditional stability constants at pH 7.4 and stability constants of the metal complexes of $\mathbf{L^1}$ and $\mathbf{L^2}$ and 298 K. log K were calculated for the formation of ML complexes.

		Cu^I	Zn^{II}	Cd^{II}	Pb^{II}
$\log K_{pH7.4}$	$\mathbf{L^1}$[19]	19.2(1)	10.3(2)	11.8(3)	10.1(1)
	$\mathbf{L^2}$	18.8(1)	11.0(2)	12.1(3)	10.5(1)
$\log K$[a]	$\mathbf{L^1}$	23.6(1)	14.6(2)	16.1(3)	14.4(1)
	$\mathbf{L^2}$	24.5(1)	16.7(2)	17.8(3)	16.2(1)

[a] $\log K$ values were calculated from $\log K_{pH7.4}$ and pK_a values according to Equations (1) and (2) in the Supporting Information.

$$Cu\text{-}\mathbf{L^i} + 2\,BCS^{2-} \rightarrow \mathbf{L^i} + [Cu(BCS)_2]^{3-} \quad (5)$$

The conditional stability constants of $\mathbf{L^1}$ and $\mathbf{L^2}$ for divalent metal ions have been measured as previously described, in Bis-Tris buffer, by analysing the direct titration of the ligand with Pb^{II} and the competition titration starting from the Pb complex for Cd^{II} and Zn^{II}.[14,42] As expected the back-titrations show endpoints at one metal equivalent. The conditional stability constant at physiological pH ($K_{pH7.4}$) and the stability constant (K) calculated from the conditional stability constants and the ligand's pK_a given in Table 1 are listed in Table 6. These data show rather similar selectivities to those obtained previously with thiol-rich ligands, that is, cysteine-containing peptides: $Cu^I \gg Cd^{II} > Pb^{II} \approx Zn^{II}$.[12,14,15] The metal complexes of $\mathbf{L^{1,2}}$ are systematically more stable than those of $\mathbf{P^C}$, which mimics Atx1 binding loop (MXCXXC sequence). It can also be noted that the stability constants of $\mathbf{L^2}$, $\log K$ in Table 6, which are not dependent on pH, are larger than the same values for $\mathbf{L^1}$, because the electron-withdrawing effect of the ester group in $\mathbf{L^1}$ is larger than the one of the amide group in $\mathbf{L^2}$. Finally, the use of three thiolates in comparison to only two thiolates in the ligand's architecture allowed us to obtain more stable Cu^I complexes, with slightly lower Cu/Zn selectivities.

Discussion

The objective of this work was the design of efficient chelators of the essential metal ion copper in the +I oxidation

state present in cells. Indeed, copper may become toxic in case of dysfunction of its homeostasis like in Wilson's disease. We previously demonstrated that small peptide sequences with two cysteine residues chelate metal ions with their two thiolate functions with a high selectivity for the soft ions Cu^{I} and Hg^{II} with respect to the three divalent cations Cd^{II}, Pb^{II} and Zn^{II}.[14,15] In particular, the selectivity with respect to Zn^{II}, which is a bioavailable ion present in cells and thus a potential competitor, is a key parameter to obtain efficient chelators in vivo.[12] We have shown here that the introduction of three cysteine residues in a tripodal architecture provides even more efficient Cu^{I} chelators with large selectivities with respect to Zn^{II}. Three tripodal molecules derived from nitrilotriacetic acid were synthesised and differ by the nature of the carbonyl function adjacent to the thiol group. Our results demonstrate that the nature of the carbonyl function has a great impact on the ligands' complexation properties. In particular, charged residues destabilise the thiolate-based metal coordination, whereas neutral groups tend to favour the formation of mononuclear Cu^{I} complexes.

The negatively charged derivative $\mathbf{L^3}$, which has three carboxylate functions close to the metal binding site, forms complexes of low stability, as seen from the BCS competition measurements. An even more striking effect is the inability of $\mathbf{L^3}$ to bind Cu^{I} in a mononuclear CuS_3 complex. Indeed only polymetallic copper(I) thiolate species were evidenced with $\mathbf{L^3}$. The destabilisation of copper(I) complexes by close carboxylate side chains of aspartate or glutamate residues has also been observed in cysteine-containing cyclodecapeptides.[12] This effect can be attributed to the large electrostatic repulsions generated by the proximate negatively charged functions which are moved closer in the metal complexes.

In contrast, the two neutral tripodal ligands $\mathbf{L^1}$ and $\mathbf{L^2}$, which bear primary amide or ester groups, form very stable mononuclear complexes of Cu^{I} with a CuS_3 geometry. Such a coordination geometry was described in the solid state in Cu^{I} complexes with monodentate sulfur ligands that were crystallised in organic solvents.[33,43] Nevertheless, to our knowledge, such complexes with a Cu^{I} metal ion coordinated by three thiolate donor groups inducing a isolated CuS_3 centre were never described in water. The complexes Cu-$\mathbf{L^1}$ and Cu-$\mathbf{L^2}$ were fully characterised by UV, CD, and ^{1}H NMR spectroscopy and ES-MS and are especially stable ($\log K \approx 19$). These affinities may be compared to the one previously determined with the cyclodecapeptide $\mathbf{P^C}$, mimicking the Atx1 binding loop, which was studied in the same conditions ($\log K = 17.4$). The introduction of three cysteines in this tripodal architecture provides Cu^{I} complexes of enhanced stability, nearly 1.5 orders of magnitude in comparison to peptides bearing two cysteines. The two tripods $\mathbf{L^1}$ and $\mathbf{L^2}$ afford three converging cysteine residues for metal complexation, which promote the coordination of Cu^{I} in a mononuclear CuS_3 geometry. Furthermore, the whole complex structure is stabilised by an intramolecular hydrogen-bonding network in the upper cavity of the tripodal molecule, which was clearly evidenced by the very low chemical-shift temperature coefficient of the amide protons. Complexes Cu-$\mathbf{L^1}$ and Cu-$\mathbf{L^2}$ exhibit rather similar conditional stability constant at physiological pH and these very large values are comparable to constants obtained with metallothioneins.[17]

A key parameter in the design of metal chelator is their selectivity with respect to bioavailable metal ions, the homeostasis of which should not be disturbed. The affinity of $\mathbf{L^{1,2}}$ for Zn^{II} is higher than those obtained with peptides bearing only two cysteines like $\mathbf{P^C}$,[14] as Zn^{II} is known to prefer sulfur-rich tetrahedral coordination sites.[42] The conditional stability constants at pH 7.4 obtained with $\mathbf{L^1}$ and $\mathbf{L^2}$ are in the same range as the one reported by Faller et al. ($\log K = 9.5$) with a peptide derived from APP and also containing three cysteine residues.[39] Even if $\mathbf{L^1}$ and $\mathbf{L^2}$ have significant affinities for Zn^{II}, their selectivities for Cu^{I} with respect to Zn^{II} remain especially large, 8–9 orders of magnitude and could be used for the selective decorporation of copper in cells.

Conclusion

In conclusion, we have developed tripodal pseudopeptide scaffolds extended by three converging cysteines, which afford soft sulfur donors for the complexation of soft metal ions. The nature of the carbonyl function next to the thiols is determinant in the complexation properties of these novel ligands. Indeed, the presence of carboxylate groups in $\mathbf{L^3}$ tends to lower the complexes' stabilities and these functions may also interfere in the coordination as it was evidenced with the borderline cation Pb^{II}. In contrast, the ester and amide derivatives $\mathbf{L^1}$ and $\mathbf{L^2}$ show interesting complexation properties. In particular, they form mononuclear Cu^{I} complexes with a unique MS_3 coordination in water, which is stabilised by a hydrogen-bonding network in the upper cavity of the tripod. The CuS_3 isolated centre is of particular interest as it is proposed as an intermediate in copper transfer in cells between copper chaperones and ATPases.[2,4,5,44] Therefore Cu-$\mathbf{L^1}$ and Cu-$\mathbf{L^2}$ may be relevant models to study this transfer, which is a key reaction in copper regulation and distribution. Besides, the introduction of three cysteines in $\mathbf{L^1}$ and $\mathbf{L^2}$ allowed us to obtain Cu^{I} chelators with very high affinities, in the same range as metallothioneins ($\log K \approx 19$).[17] Moreover, these ligands display large selectivities for the targeted metal ion Cu^{I} with respect to bioavailable Zn^{II}, which is critical to obtain efficient decorporation agents in vivo that do not alter essential ion homeostasis.

Experimental Section

General: Solvents and starting materials were purchased from Aldrich, Acros, Fluka and Alfa Aesar and used without further purification. HCys(Trt)OEt was synthesised according to a published procedure.[45] All solutions in water were prepared from ultrapure laboratory grade water

that has been filtered and purified by reverse osmosis using Millipore MilliQ reverse-osmosis cartridge system (resistivity 18 MΩ cm). Thin-layer chromatography (TLC) was performed on silica gel 60 F254 (Merck). Flash chromatography was performed on silica gel 60 (40–63 μm, Merck). Analytical and preparative HPLC was performed with a VWR system fitted with a purosphere RP18 column ($l=250$ mm, $Ø=4.6$ mm and $p=5$ μm for analytical column; $l=250$ mm, $Ø=40$ mm and $p=10$ μm for preparative column). Solvent conditions were as follows: solvent A = water/TFA (99.925:0.075), solvent B = CH_3CN/water/TFA (90:10:0.1). Flow rates of 1 mL min^{-1} and 75 mL min^{-1} were used for analytical and preparative column respectively with UV monitoring at 214 nm. ^{1}H NMR and ^{13}C NMR spectra were recorded on a Mercury Varian 400 spectrometer or on a Bruker 500 spectrometer. Chemical shifts are reported in ppm with the solvent as the internal reference. Mass spectra were acquired with a Finigan LCQ-ion trap equipped with an electrospray source. Elemental analyses were performed by the Service Central d'Analyse (Solaize, France).

Synthesis of compound 1: Nitrilotriacetic acid (0.196 g, 1.03 mmol) was added to a solution of HCys(Trt)OEt (1.200 g, 3.06 mmol) in DMF (20 mL). Then the mixture was cooled at 0 °C and *N*-ethyl-*N*′-(3-dimethylaminopropyl)carbodiimide (0.587 g, 3.06 mmol) and 1-hydroxybenzotriazole hydrate (0.414 g, 3.06 mmol) were successively added. The reaction mixture was stirred at room temperature for 24 h under argon. After evaporation of the solvent, the residue was dissolved in ethyl acetate (100 mL). The organic layer was washed with water (2×50 mL), saturated $NaHCO_3$ solution (50 mL) and brine (2×50 mL). The organic layer was dried over Na_2SO_4 and concentrated under reduced pressure. The resulting crude product (1.391 g) was purified by column chromatography on silica gel (100 mL, CH_2Cl_2/ethyl acetate, 80:20) to give compound **1** (1.103 g, 82 %) as a white powder. ^{1}H NMR (CD_3CN, 400 MHz, 298 K): $\delta=1.05$ (t, $J=7.0$ Hz, 9H; CH_3), 2.39 and 2.68 (ABX, $J_{BX}=4.1$ Hz, $J_{AX}=8.0$ Hz, $J_{AB}=12.7$ Hz, 6H; CH_2S), 3.17 and 3.29 (AB, $J_{AB}=15.0$ Hz, 6H; CH_2CO), 3.84 and 3.96 (ABX$_3$, $J_{AX}=7.0$ Hz, $J_{BX}=7.0$ Hz, $J_{AB}=10.9$ Hz, 6H; CH_2CH$_3$), 4.34 (td, $J=4.0$, 8.2 Hz, 3H; C*H*), 7.13–7.17 (m, 30H; SC(C$_6H_5$)$_3$), 7.22 (d, $J=7.4$ Hz, 15H; SC(C$_6H_5$)$_3$), 7.56 ppm (d, $J=8.6$ Hz, 3H; N*H*); ^{13}C NMR (CD_3CN, 100 MHz, 298 K): $\delta=14.39$ (*C*H$_3$), 33.69 (*C*H$_2$S), 52.11 (*C*H), 57.97 (*C*H$_2$CO), 62.21 (*C*H$_2$CH$_3$), 129.90–127.16 (*C*$_6$H$_5$), 144.70 (*C*(C$_6$H$_5$)$_3$), 171.66 and 170.70 ppm (2*C*O); ES-MS: m/z: 1310.8 $[M+H]^+$; elemental analysis calcd (%) for $C_{78}H_{78}N_4O_9S_2{\cdot}2H_2O$ (1347.70 g mol^{-1}): C 69.51, H 6.13, N 4.16; found: C 69.42, H 6.05, N 3.90.

Synthesis of compound 2: Nitrilotriacetic acid (0.068 g, 0.357 mmol) was added to a solution of HCys(Trt)(NH_2) (0.401 g, 1.10 mmol) in DMF (10 mL). Then the mixture was cooled at 0 °C and *N*-ethyl-*N*′-(3-dimethylaminopropyl)carbodiimide (0.212 g, 1.10 mmol) and 1-hydroxybenzotriazole hydrate (0.150 g, 1.11 mmol) were successively added. The reaction mixture was stirred at room temperature for 24 h under argon. After evaporation of the solvent, the residue was washed with water (25 mL) and filtrated. Then the solid was dissolved in dichloromethane (100 mL) and the organic layer was washed with water (3×50 mL) and brine (1×50 mL). The organic layer was dried over Na_2SO_4 and concentrated under reduced pressure to give the compound **2** (0.404 g, 92 %) as a white powder. ^{1}H NMR (CD_3CN, 400 MHz, 298 K): $\delta=2.37$–2.44 (m, 6H; CH_2S), 3.14 and 3.19 (AB, $J_{AB}=16.4$, 6H; CH_2CO), 4.00–4.06 (m, 3H; C*H*), 5.70 (s, 3H; NH_2), 6.24 (s, 3H; NH_2), 7.16–7.32 (m, 45H; SC(C$_6H_5$)$_3$), 7.85 ppm (d, $J=7.2$, 3H; N*H*); ^{13}C NMR (CD_3CN, 100 MHz, 298 K): $\delta=38.89$ (*C*H$_2$SH), 57.78 (*C*H), 63.18 (*C*H$_2$CO), 132.37–134.89 ((*C*$_6$H$_5$)$_3$), 150.03 (*C*(C$_6$H$_5$)$_3$), 176.15 and 178.074 ppm (2*C*O); ES-MS: m/z: 1223.8 $[M+H]^+$; elemental analysis calcd (%) for $C_{72}H_{69}N_7O_6S_3{\cdot}H_2O$ (1242.57 g mol^{-1}): C 69.60, H 5.76, N 7.89; found: C 69.60, H 5.72, N, 7.95

Synthesis of compound 3: Compound **1** (0.310, 0.236 mmol) was dissolved in ethanol (6 mL) and LiOH (1 M, 0.95 mL, 0.95 mmol) was added. The reaction mixture was stirred at room temperature for 1 h. Then, the reaction mixture was evaporated and the residue was dissolved in water (6 mL) and HCl (1 M) was added until pH 4–5. The aqueous layer was extracted with ethyl acetate (15 mL). The organic layer was dried over Na_2SO_4 and concentrated under reduced pressure. The resulting crude product (0.242 mg, 83 %) was used without further purification. ^{1}H NMR ([D$_6$]DMSO, 400 MHz, 298 K): $\delta=2.37$–2.46 (m, 6H; CH_2SC), 3.32 (s, 6H; CH_2CO), 4.17–4.21 (m, 3H; C*H*), 7.20–7.37 (m, 45H; C(C$_6H_5$)$_3$), 8.46 ppm (d, $J=7.4$ Hz, 3H; N*H*); ^{13}C NMR (CD_3CN, 100 MHz, 298 K): $\delta=34.03$ (*C*H$_2$S), 52.34 (*C*H), 60.68 (*C*H$_2$CO), 130.00–127.67 ((*C*$_6$H$_5$)$_3$), 145.16 (*C*(C$_6$H$_5$)$_3$), 172.02 and 171.61 ppm (2*C*O); ES-MS: m/z: =1249.2 $[M+Na]^+$.

Synthesis of ligand L^1: Trifluoroacetic acid (1.81 mL, 24.4 mmol) and triethylsilane (0.47 mL, 2.9 mmol) were successively added to a solution of **1** (0.640 g, 0.49 mmol) in CH_2Cl_2 (15 mL) under argon. After stirring for 30 min at room temperature, the mixture was evaporated. The resulting crude product (0.627 mg) was purified by preparative HPLC ($t_R=12.7$ min ; linear gradient 50:50 to 0:100, A/B in 15 min; analytical HPLC: $t_R=7.1$ min with the same gradient). Ligand **L^1** was obtained as a white oily solid (0.110 g, 49 %). ^{1}H NMR (CD_3CN, 500 MHz, 298 K): $\delta=1.25$ (t, $J=7.1$ Hz, 9H; CH_3), 1.97 (t, $J=8.8$ Hz, 3H; S*H*), 2.95 and 3.00 (ABXY, $J_{AX}=4.6$ Hz, $J_{BX}=6.1$ Hz, $J_{BY}=9.0$, $J_{AY}=9.3$ Hz, $J_{AB}=14.0$ Hz, 6H; CH_2SH), 3.48 and 3.52 (AB, $J_{AB}=16.3$ Hz, 6H; CH_2CO), 4.18 and 4.22 (ABX$_3$; $J_{AX}=7.1$ Hz, $J_{BX}=7.1$ Hz, $J_{AB}=10.8$ Hz, 6H; CH_2-CH$_3$), 4.70 (ddd, $J=4.7$, 6.2, 8.0 Hz, 3H; C*H*), 7.71 ppm (d, $J=8.0$ Hz, 3H; N*H*); ^{13}C NMR (CD_3CN, 100 MHz, 298 K): $\delta=14.97$ (*C*H$_3$), 27.40 (*C*H$_2$SH), 55.81 (*C*H), 59.75 (*C*H$_2$CO), 63.02 (*C*H$_2$CH$_3$), 171.61 and 172.02 ppm (2*C*O); ES-MS: m/z: =585.0 $[M+H]^+$, 607.3 $[M+Na]^+$.

Synthesis of ligand L^2: Trifluoroacetic acid (1.4 mL, 17.84 mmol) and triethylsilane (0.54 mL, 2.14 mmol) were successively added to a solution of **2** (0.437 g, 0.357 mmol) in CH_2Cl_2 (15 mL) under argon. After stirring for 50 min at room temperature, the mixture was evaporated. The resulting crude product (0.6 mg) was purified by preparative HPLC ($t_R=18.9$ min linear gradient from 95:5 to 65:35, A/B in 25 min; analytical HPLC: $t_R=16.4$ min with the same gradient) and gave the compound **L^2** (0.065 g, 37 %) as a white solid. ^{1}H NMR (D_2O, 500 MHz, 298 K): $\delta=2.87$ (ABX, $J_{AX}=4.9$ Hz, $J_{BX}=7.5$ Hz, $J_{AB}=14.2$ Hz, 6H; CH_2SH), 3.55 (s, 6H; CH_2CO), 4.45 ppm (dd, $J=7.5$, 4.9 Hz, 3H; C*H*); ^{13}C NMR (D_2O, 100 MHz, 298 K): $\delta=28.18$ (*C*H$_2$SH) ; 57.93 (*C*H), 60.85 (*C*H$_2$CO), 175.98 and 177.04 ppm (2*C*O); ES-MS: m/z: 498.1 $[M+H]^+$.

Synthesis of ligand L^3: Trifluoroacetic acid (1.77 mL, 23.8 mmol) and triethylsilane (0.456 mL, 2.85 mmol) were successively added to a solution of **3** (0.584 g, 0.476 mmol) in CH_2Cl_2 (21 mL), under argon. After stirring for 30 min at room temperature, the mixture was evaporated. The resulting crude product (744.5 mg) was purified by preparative HPLC ($t_R=13.75$ min ; linear gradient 95:5 to 0:100, A/B in 15 min; analytical HPLC: $t_R=12.5$ min with the same gradient). Ligand **L^3** was obtained as a white powder (0.209 g, 88 %). ^{1}H NMR (D_2O, 400 MHz, 298 K): $\delta=3.07$ and 3.01 (ABX, $J_{AX}=4.3$ Hz, $J_{BX}=6.8$ Hz, $J_{AB}=14.5$ Hz, 6H; CH_2SH), 3.81–3.90 (m, 6H; CH_2CO), 4.72 ppm (t, $J=5.9$ Hz, 3H; C*H*); ^{13}C NMR (CD_3CN, 100 MHz, 298 K): $\delta=27.86$ (*C*H$_2$SH), 57.38 (*C*H), 60.07 (*C*H$_2$CO), 173.46 (*C*OOH), 175.77 ppm (NH*C*O); ES-MS: m/z: 499.0 $[M-H]^-$.

Compounds **L^1**, **L^2** and **L^3** are sensitive to air-oxidation. Therefore they were stored and manipulated in a glove box (Argon, $O_2<0.1$ ppm).

Solution preparation: Since the cysteine residues in the chelators are susceptible to air oxidation, all the solutions were prepared in a glove box under argon atmosphere. Fresh solutions of the ligand were prepared before each experiment, using the appropriate buffer prepared with deoxygenated Milli-Q® water (Millipore) and acetonitrile. Solutions of **L^1** were systematically prepared with 10 % acetonitrile (vol), except for potentiometry experiments for which only 2 % acetonitrile (vol) were used. Solutions of **L^{2,3}** were prepared with 10 % acetonitrile (vol) for copper titrations to avoid copper(I) disproportionation or for NMR samples to use the residual signal of CD_2HCN as an internal reference. For other experiments solutions of **L^{2,3}** were prepared without acetonitrile.

The final concentration of the ligand solutions were determined by measuring the cysteine free-thiol concentration following the Ellman's procedure.[28] This procedure uses 5,5′-dithiobis-2-nitrobenzoic acid (DTNB) as an indicator: each free thiol group present in the peptide yields one equivalent of TNB^{2-} ($\varepsilon_{412\,nm}$ (TNB^{2-}) = 14 150 M^{-1} cm^{-1}).

Solutions of Cu^I were prepared by dissolving the appropriate amount of $Cu(CH_3CN)_4PF_6$ in deoxygenated acetonitrile. The final concentration

was determined by adding an excess of sodium bathocuproine disulfonate (Na_2BCS) and measuring the absorbance of $[Cu(BCS)_2]^{3-}$ ($\lambda_{max}=483$ nm, $\varepsilon=13\,300\,M^{-1}cm^{-1}$).

The other metal solutions were prepared from the corresponding salt ($CdCl_2$, $PbCl_2$ or $ZnCl_2$) in water or in the appropriate buffer and titrated by 5 mM volumetric EDTA (Fisher Chemicals) in presence of a colourimetric indicator.

Potentiometry: All titrant solutions were prepared using water purified by passing through a Millipore Milli-Q reverse-osmosis cartridge system (resistivity 18 MΩ cm). Carbonate-free 0.1 mol L^{-1} KOH and 0.1 mol L^{-1} HCl were prepared from Fisher Chemicals concentrates. Potentiometric titrations were performed in 0.1 mol L^{-1} aqueous KCl in the glove box to avoid oxidation of the thiol groups into disulfide, the temperature was controlled to ±0.1 °C with a circulating water bath. The p[H] (p[H] = −log[H^+], concentration in molarity) was measured in each titration with a combined pH glass electrode (Metrohm) filled with 3 mol L^{-1} KCl and the titrant addition was automated by use of a 751 GPD titrino (Metrohm). The electrode was calibrated in hydrogen ion concentration by titration of HCl with KOH in 0.1 mol L^{-1} KCl.[46] A plot of meter reading versus p[H] allows the determination of the electrode standard potential ($E°$) and the slope factor (f). Continuous potentiometric titrations with KOH 0.1 mol L^{-1} were conducted on 22 mL of aqueous solutions containing 0.5 10^{-3} mol L^{-1} of the ligand. Back titrations with HCl 0.1 mol L^{-1} were systematically performed after each experiment to check whether equilibration had been achieved. In a typical experiment, 100 points were measured with a 2 min delay between the measurements.

Experimental data were refined using the computer program Hyperquad 2000.[47] All equilibrium apparent constants are expressed as concentration ratio and not activities. The ionic product of water at 25 °C and 0.1 mol L^{-1} ionic strength is $pK_w=13.78$.[48] The initial concentrations of ligands were fixed.

UV and CD titrations: The UV/Vis spectra were recorded with a Varian Cary50 spectrophotometer equipped with optical fibres connected to an external cell holder in the glove box. The circular dichroism spectra were acquired with an Applied Photophysics Chirascan spectrometer. CD spectra are reported in molar ellipticity ([Θ] in units of deg cm^2 mol^{-1}). $[\Theta]=\theta_{obs}/(10lc)$, in which θ_{obs} is the observed ellipticity in millidegrees, l the optical path length of the cell in centimeters, c the peptide concentration in moles per litre.

A 2–2.5 mL portion of the ligand solution (≈ 50 μM) was transferred in a cell (1 cm path) and aliquots of the metal solution were then added. The buffer was phosphate (20 mM, pH 7.4) for all the titrations except for Pb^{II} for which Bis-Tris (20 mM, pH 7) was used to prevent Pb^{II} hydrolysis and the precipitation of $Pb(OH)_2$.[42]

ESI-MS titrations: Mass spectra were acquired on a LXQ-linear ion trap (THERMO Scientific, San Jose, USA) equipped with an electrospray source. Electrospray full scan spectra in the range $m/z=150$–2000 amu were obtained by infusion through a fused silica tubing at 2–10 μL min^{-1}. The solutions were analysed in the negative and positive modes. The LXQ calibration ($m/z=50$–2000) was achieved according to the standard calibration procedure from the manufacturer (mixture of caffeine, MRFA and Ultramark 1621). The temperature of the heated capillary for the LXQ was set to 180–200 °C, the ion-spray voltage was in the range 2–4 kV and the injection time was 10–100 ms. The ligand solution (100 μM) was prepared in ammonium acetate buffer (20 mM, pH 7)/acetonitrile (v/v=9:1) and aliquots of the metal solution were then added.

^{1}H NMR spectroscopy: The NMR experiments were recorded on a 500 MHz Bruker Avance spectrometer equipped with a BBI probe with triple axis gradient field. ^{1}H NMR spectra were recorded with 12 ppm windows and 32 k data points in the time domain. Ligand samples prepared in phosphate buffer 20 mM pH 7.4 in D_2O/CD_3CN (v/v = 9/1) with a ≈1 mM concentration, were titrated with aliquots of a $Cu(CH_3CN)_4PF_6$ solution in CD_3CN or a divalent metal ion solution in D_2O.

Diffusion coefficient measurement were performed using the bipolar stimulated spin echo sequence.[49] Diffusion coefficients were obtained using, $I(\delta,\Delta,g)=I_0\exp[-\gamma^2g^2\delta^2(\Delta-\delta/3)D]$, $I(\delta,\Delta,g)$ and I_0 are the intensities in the presence of gradient pulses of strength g and in absence of gradient pulses respectively. The length of the gradient pulse is δ, Δ is the diffusion delay and γ is the gyromagnetic ratio (for protons, $\gamma_H=26.7520\times10^7$ rad.T^{-1} s^{-1}). The values of Δ and δ used in the diffusion coefficient measurements were 100 ms and 2 ms respectively. In the experiments g was incremented from 2.95 to 47.2 G cm^{-1}.

The temperature coefficients of the amide proton resonances of the copper complexes were measured in phosphate buffer (20 mM, pH 7.4)/CD_3CN, 90/10 (v/v) using watergate water suppression, and the signal of CD_2HCN as an internal reference.

Affinity constants: See Supporting Information for details.

Acknowledgements

We thank Yves Chenavier for performing some of the titration experiments and Pierre-Alain Bayle for his help in acquiring NMR data. The financial support from the Cluster de recherche Chimie de la Région Rhône-Alpes is duly acknowledged.

[1] a) R. H. Holm, P. Kennepohl, E. I. Solomon, *Chem. Rev.* **1996**, *96*, 2239–2314; b) S. Tottey, D. R. Harvie, N. J. Robinson, *Acc. Chem. Res.* **2005**, *38*, 775–783; c) P. P. Kulkarni, Y. M. She, S. D. Smith, E. A. Roberts, B. Sarkar, *Chem. Eur. J.* **2006**, *12*, 2410–2422.
[2] L. A. Finney, T. V. O'Halloran, *Science* **2003**, *300*, 931–936.
[3] a) N. J. Robinson, D. R. Winge, *Annu. Rev. Biochem.* **2010**, *79*, 537–562; b) B. E. Kim, T. Nevitt, D. J. Thiele, *Nat. Chem. Biol.* **2008**, *4*, 176–185.
[4] F. Arnesano, L. Banci, I. Bertini, S. Ciofi-Baffoni, *Eur. J. Inorg. Chem.* **2004**, 1583–1593.
[5] A. C. Rosenzweig, *Acc. Chem. Res.* **2001**, *34*, 119–128.
[6] S. Puig, D. J. Thiele, *Curr. Opin. Chem. Biol.* **2002**, *6*, 171–180.
[7] T. Y. Tao, J. A. Gitlin, *Hepatology* **2003**, *37*, 1241–1247.
[8] B. Sarkar, *Chem. Rev.* **1999**, *99*, 2535–2544.
[9] A. I. Bush, *Trends Neurosci.* **2003**, *26*, 207–214.
[10] a) E. Gaggelli, H. Kozlowski, D. Valensin, G. Valensin, *Chem. Rev.* **2006**, *106*, 1995–2044; b) P. S. Donnelly, Z. G. Xiao, A. G. Wedd, *Curr. Opin. Chem. Biol.* **2007**, *11*, 128–133; c) P. Faller, C. Hureau, *Dalton Trans.* **2009**, 1080–1094.
[11] a) O. Andersen, *Chem. Rev.* **1999**, *99*, 2683–2710; b) K. L. Haas, K. J. Franz, *Chem. Rev.* **2009**, *109*, 4921–4960; c) L. R. Perez, K. J. Franz, *Dalton Trans.* **2010**, *39*, 2177–2187.
[12] A. M. Pujol, M. Cuillel, O. Renaudet, C. Lebrun, P. Charbonnier, D. Cassio, C. Gateau, P. Dumy, E. Mintz, P. Delangle, *J. Am. Chem. Soc.* **2011**, *133*, 286–296.
[13] a) A. C. Rosenzweig, T. V. O'Halloran, *Curr. Opin. Chem. Biol.* **2000**, *4*, 140–147; b) S. J. Opella, T. M. DeSilva, G. Veglia, *Curr. Opin. Chem. Biol.* **2002**, *6*, 217–223; c) F. Arnesano, L. Banci, I. Bertini, S. Ciofi-Baffoni, E. Molteni, D. L. Huffman, T. V. O'Halloran, *Genome Res.* **2002**, *12*, 255–271.
[14] P. Rousselot-Pailley, O. Sénèque, C. Lebrun, S. Crouzy, D. Boturyn, P. Dumy, M. Ferrand, P. Delangle, *Inorg. Chem.* **2006**, *45*, 5510–5520.
[15] O. Sénèque, S. Crouzy, D. Boturyn, P. Dumy, M. Ferrand, P. Delangle, *Chem. Commun.* **2004**, 770–771.
[16] K. A. Koch, M. M. O. Pena, D. J. Thiele, *Chem. Biol.* **1997**, *4*, 549–560; M. J. Stillman, *Coord. Chem. Rev.* **1995**, *144*, 461–511.
[17] P. Faller, *Febs J.* **2010**, *277*, 2921–2930.
[18] V. Calderone, B. Dolderer, H. J. Hartmann, H. Echner, C. Luchinat, C. Del Bianco, S. Mangani, U. Weser, *Proc. Natl. Acad. Sci. USA* **2005**, *102*, 51–56.
[19] A. M. Pujol, C. Gateau, C. Lebrun, P. Delangle, *J. Am. Chem. Soc.* **2009**, *131*, 6928–6929.
[20] M. Gelinsky, R. Vogler, H. Vahrenkamp, *Inorg. Chem.* **2002**, *41*, 2560–2564.
[21] C. Jeunesse, D. Armspach, D. Matt, *Chem. Commun.* **2005**, 5603–5614.

[22] a) M. Heitzmann, C. Gateau, L. Chareyre, M. Miguirditchian, M.-C. Charbonnel, P. Delangle, *New J. Chem.* **2010**, *34*, 108–116; b) M. Heitzmann, F. Bravard, C. Gateau, N. Boubals, C. Berthon, J. Pecaut, M. C. Charbonnel, P. Delangle, *Inorg. Chem.* **2009**, *48*, 246–256; c) A. Pellissier, Y. Bretonniere, N. Chatterton, J. Pecaut, P. Delangle, M. Mazzanti, *Inorg. Chem.* **2007**, *46*, 3714–3725; d) F. Bravard, C. Rosset, P. Delangle, *Dalton Trans.* **2004**, 2012–2018; e) F. Bravard, Y. Bretonniere, F. Wietzke, C. Gateau, M. Mazzanti, P. Delangle, J. Pecaut, *Inorg. Chem.* **2003**, *42*, 7978–7989.
[23] C. J. Siddons, R. D. Hancock, *Chem. Commun.* **2004**, 1632–1633.
[24] R. Vogler, M. Gelinsky, L. F. Guo, H. Vahrenkamp, *Inorg. Chim. Acta* **2002**, *339*, 1–8.
[25] P. Kamau, R. B. Jordan, *Inorg. Chem.* **2001**, *40*, 3879–3883.
[26] D. L. Pountney, I. Schauwecker, J. Zarn, M. Vasak, *Biochemistry* **1994**, *33*, 9699–9705.
[27] P. Faller, M. Vasak, *Biochemistry* **1997**, *36*, 13341–13348.
[28] P. W. Riddles, R. L. Blakeley, B. Zerner, *Methods Enzymol.* **1983**, *91*, 49–60.
[29] M. Karplus, *J. Am. Chem. Soc.* **1963**, *85*, 2870–2871.
[30] A. R. Waldeck, P. W. Kuchel, A. J. Lennon, B. E. Chapman, *Prog. Nucl. Magn. Reson. Spectrosc.* **1997**, *30*, 39–68.
[31] a) M. Alajarín, A. Pastor, R.-A. Orenes, E. Martinez-Viviente, P. S. Pregosin, *Chem. Eur. J.* **2006**, *12*, 877–886; b) E. Terazzi, S. Torelli, G. Bernardinelli, J.-P. Rivera, J.-M. Bénech, C. Bourgogne, B. Donnio, D. Guillon, D. Imbert, J.-C. G. Bünzli, A. Pinto, D. Jeanneraat, C. Piguet, *J. Am. Chem. Soc.* **2005**, *127*, 888–903.
[32] a) E. Schievano, A. Bisello, M. Chorev, A. Bisol, S. Mammi, E. Peggion, *J. Am. Chem. Soc.* **2001**, *123*, 2743–2751; b) H. Kessler, *Angew. Chem.* **1982**, *94*, 509–520; *Angew. Chem. Int. Ed. Engl.* **1982**, *21*, 512–523; c) H. J. Dyson, M. Rance, R. A. Houghten, R. A. Lerner, P. E. Wright, *J. Mol. Biol.* **1988**, *201*, 161–200.
[33] C. D. Garner, J. R. Nicholson, W. Clegg, *Inorg. Chem.* **1984**, *23*, 2148–2150.
[34] G. A. Jeffrey, *An Introduction to Hydrogen Bonding*, Oxford University Press, New York, **1997**.
[35] a) K. B. Nielson, C. L. Atkin, D. R. Winge, *J. Biol. Chem.* **1985**, *260*, 5342–5350; b) A. Presta, A. R. Green, A. Zelazowski, M. J. Stillman, *Eur. J. Biochem.* **1995**, *227*, 226–240.
[36] J. S. Magyar, T.-C. Weng, C. M. Stern, D. F. Dye, B. W. Rous, J. C. Payne, B. Bridgewater, A. M. Mijovilovich, G. Parkin, J. M. Zaleski, J. E. Penner-Hahn, H. A. Godwin, *J. Am. Chem. Soc.* **2005**, *127*, 9495–9505.
[37] M. Matzapetakis, B. T. Farrer, T.-C. Weng, L. Hemmingsen, J. E. Penner-Hahn, V. L. Pecoraro, *J. Am. Chem. Soc.* **2002**, *124*, 8042–8054.
[38] C. J. Henehan, D. L. Poutney, O. Zerbe, M. Vasak, *Protein Sci.* **1993**, *2*, 1756–1764.
[39] E.-D. Ciuculescu, Y. Mekmouche, P. Faller, *Chem. Eur. J.* **2005**, *11*, 903–909.
[40] Z. Xiao, F. Loughlin, G. N. George, G. J. Howlett, A. G. Wedd, *J. Am. Chem. Soc.* **2004**, *126*, 3081–3090.
[41] R. Miras, I. Morin, O. Jacquin, M. Cuillel, F. Guillain, E. Mintz, *J. Biol. Inorg. Chem.* **2008**, *13*, 195–205.
[42] J. C. Payne, M. A. terHorst, H. A. Godwin, *J. Am. Chem. Soc.* **1999**, *121*, 6850–6855.
[43] D. Coucouvanis, C. N. Murphy, S. K. Kanodia, *Inorg. Chem.* **1980**, *19*, 2993–2998; S. Zeevi, E. Y. Tshuva, *Eur. J. Inorg. Chem.* **2007**, 5369–5376.
[44] a) R. A. Pufahl, C. P. Singer, K. L. Peariso, S.-J. Lin, P. J. Schmidt, C. J. Fahrni, V. C. Culotta, J. E. Penner-Hahn, T. V. O'Halloran, *Science* **1997**, *278*, 853–856; b) A. K. Wernimont, D. L. Huffman, A. L. Lamb, T. V. O'Halloran, A. C. Rosenzweig, *Nat. Struct. Biol.* **2000**, *7*, 766–771; c) A. Rodriguez-Granillo, A. Crespo, D. A. Estrin, P. Wittung-Stafshede, *J. Phys. Chem. B* **2010**, *114*, 3698–3706.
[45] C. Bolzati, A. Mahmood, E. Malago, L. Uccelli, A. Boschi, A. G. Jones, F. Refosco, A. Duatti, F. Tisato, *Bioconjugate Chem.* **2003**, *14*, 1231–1242.
[46] A. E. Martell and R. J. Motekaitis, *Determination and Use of Stability Constants*, VCH, Weinheim, **1992**.
[47] a) P. Gans, A. Sabatini, A. Vacca, *Talanta* **1996**, *43*, 1739–1753; b) L. Alderighi, P. Gans, A. Ienco, D. Peters, A. Sabatini, A. Vacca, *Coord. Chem. Rev.* **1999**, *184*, 311–318.
[48] R. M. Smith, A. E. Martell, R. J. Motekaitis, NIST Critically Selected Stability Constants of Metal Complexes Database, NIST Standard Reference Database 46, **2001**.
[49] A. Jerschow, N. Müller, *J. Magn. Reson.* **1997**, *125*, 372–375.

Received: December 14, 2010
Published online: March 17, 2011

